Model, prediction, and experimental verification of composition and thickness in continuous spread thin film combinatorial libraries grown by pulsed laser deposition

N. D. Bassim, P. K. Schenck, and M. Otani
Materials Science and Engineering Laboratory, National Institute of Standards and Technology, Gaithersburg, Maryland 20899

H. Oguchi
Department of Materials Science and Engineering, University of Maryland, College Park, Maryland 20742

(Received 5 January 2007; accepted 7 May 2007; published online 11 July 2007)

Pulsed laser deposition was used to grow continuous spread thin film libraries of continuously varying composition as a function of position on a substrate. The thickness of each component that contributes to a library can be empirically modeled to a bimodal cosine power distribution. We deposited ternary continuous spread thin film libraries from Al_2O_3, HfO_2, and Y_2O_3 targets, at two different background pressures of O_2: 1.3 and 13.3 Pa. Prior to library deposition, we deposited single component calibration films at both pressures in order to measure and fit the thickness distribution. Following the deposition and fitting of the single component films, we predict both the compositional coverage and the thickness of the libraries. Then, we map the thickness of the continuous spread libraries using spectroscopic reflectometry and measure the composition of the libraries as a function of position using mapping wavelength-dispersive spectrometry (WDS). We then compare the compositional coverage of the libraries and observe that compositional coverage is enhanced in the case of 13.3 Pa library. Our models demonstrate linear correlation coefficients of 0.98 for 1.3 Pa and 0.98 for 13.3 Pa with the WDS. © *2007 American Institute of Physics.* [DOI: 10.1063/1.2755783]

INTRODUCTION

Combinatorial methodology is a powerful material research technique.[1–3] It involves systematically changing a process variable (i.e., material composition, film thickness, process temperature for fabrication, etc.) and fabricating a series of samples as a function of that parameter. A series of property measurements is then made in parallel, in order to (a) identify structure-property trends and (b) to act as a screening tool for further optimization and experimentation. The film, which contains the parameter variation, is called a library. Two types of libraries are possible: *discrete* and *continuous spread* libraries. Discrete libraries are designed so that each subsample in the library is a homogeneous data point, i.e., in the case of a compositionally varied library, a distinct chemical composition. The amount of data obtainable is limited by the step size between discrete compositions and the total number of discrete subsamples. In the continuous spread technique, the processing variable varies continuously across the parametric space. In this case, the amount and quality of data that are achievable are limited by the change in the variable across the dimensions of the probe size of the characterization tool and by the number of data points (inversely proportional to the measurement length) that the characterization tool can measure in a reasonable time.

Continuous spread combinatorial techniques can be divided into two categories: natural spread and artificial spread. We utilize a natural spread technique, which relies on the change in composition to occur because of the deposition pattern that occurs during growth. In artificial spread techniques, a moving aperture or shutter may be used to confine the deposition process in a more organized manner, leaving the library addressable.[4] Nevertheless, the natural spread configuration can be spread over larger areas (in our case a 76.2 mm diameter wafer), gas flow interference around a shutter can be mitigated, and reactions with the shutter during deposition can be avoided.

Our apparatus is equipped to fabricate continuous spread combinatorial libraries using pulsed laser deposition (PLD), which vary in composition and thickness continuously across a 76.2 mm wafer. Pulsed laser deposition is a technique in which a short-duration laser pulse (25 ns) strikes a ceramic target in a reduced pressure atmosphere, causing a plume of material to be ejected from the target surface initially as a plasma. This method for fabrication of film libraries is similar to that previously described by Christen *et al.*[5] The method takes advantage of the nonuniform and nonlinear deposition rate characteristic of the PLD process.

Figure 1 is a photograph that shows a typical deposition pattern of a single target PLD film (in this case HfO_2) grown on a 76.2 mm Si wafer, exhibiting an uneven thickness distribution. It should be noted here that the films were photographed from ≈45° angle in order to reduce glare from the wafer. It is well known that the PLD thickness distribution can be approximated using the following equation when the laser spot is rectangular:[6]

 © 2007 American Institute of Physics

Downloaded 28 May 2008 to 129.6.180.72. Redistribution subject to AIP license or copyright; see http://rsi.aip.org/rsi/copyright.jsp

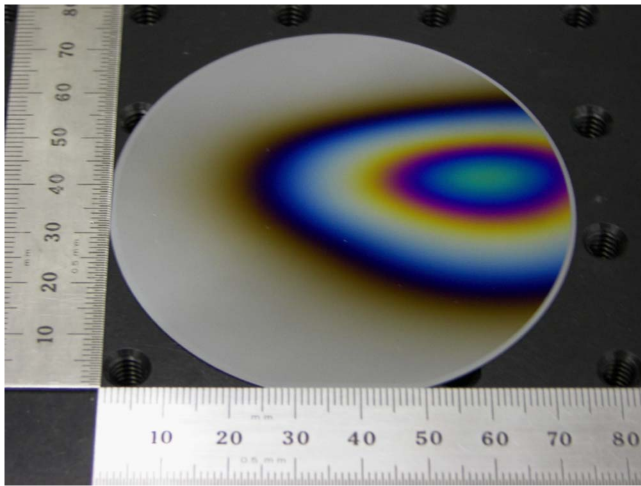

FIG. 1. (Color online) Typical calibration HfO_2 film grown at 13.3 Pa.

$$T(x,y) = T_0 \cos^m \theta_x \cos^n \theta_y, \quad (1)$$

where T_0 is the maximum thickness at the center of the pattern, θ_x and θ_y are the angles in x and y of divergence of the material plume from the centerline of the target, and m and n are power coefficients of the rates of decrease in the thickness of the film in x and y. The x coordinate is defined on the substrate as parallel to the [100] flat, and y is perpendicular to it. The origin of the x-y coordinate access is located at the point where T_0 is a maximum. The angle of divergence θ_{xi} may be defined for the ith point on the wafer x_i as

$$\theta_{xi} = \arctan\left(\frac{x_i}{z}\right), \quad (2)$$

where z is the distance between the substrate and the target. $\cos^m(\theta_x)$ may then be expressed as

$$\cos^m \theta_{xi} = \left(\frac{z}{\sqrt{z^2 + x_i^2}}\right)^m \quad (3)$$

for the x direction and as

$$\cos^n \theta_{y_j} = \left(\frac{z}{\sqrt{z^2 + y_j^2}}\right)^n \quad (4)$$

for the y direction.

This model is useful for describing the thickness distribution of a single component film. In order to fabricate combinatorial libraries, the targets must be changed and the film must be rotated to another angle to provide a continuously changing composition.

We rotate the substrate during growth to positions of 0°, 120°, and 240° and also change the target composition for a set of laser pulses at each position. We are able to fabricate mixed composition continuous spread libraries across the wafer. Each deposition step (i.e., the set of pulses) is designed so as to deposit (on average) a submonolayer thick film, in order to ensure full mixing of each layer during growth (to avoid segregation of materials into a multilayer structure). This set of growths is repeated in series in order to obtain a combinatorial library of the desired thickness.

In order to design libraries that cover a large ternary composition range, it is important to be able to predict the deposition pattern that would result from the growth, using the model described above. To do this, we must measure the thickness of three single-composition calibration films prior to growth of the library and fit them to the model of Eq. (1) with reasonable values of n and m. To test the validity of the model, we must also compare the predicted film thickness and composition to experimental data to ensure that this distribution model is valid.

Finally, we seek to demonstrate that a desired compositional coverage can be designed by changing the values of n and m. We will demonstrate that the values of n and m have significant effects on the extent of compositional coverage that is achievable. One method of manipulating the cosine distribution is by changing the scattering of the ablated material through control of the background gas pressure in the system. At low background gas partial pressures, the amount of material scattering is confined to the plume, and the deposited material emerges with fewer collisions and consequently a tighter angular spread (i.e., a higher n and m), and a higher on-axis growth rate. In addition, the deposition pattern tends to resemble the laser spot shape.[6] At higher background pressures, the background gas scatters the plume material more diffusely, causing a lower on-axis deposition rate with a wider angular spread. We will demonstrate these effects and use a simulation to predict the compositional coverage and thickness at each point in the library film as a function of background gas pressure.

EXPERIMENT

For each library, we deposited a series of single-composition calibration films to determine the growth rate and thickness distribution. We grew each film at the wafer rotation position that was later used for the fabrication of the libraries. Our test material system was the $HfO_2-Al_2O_3-Y_2O_3$ ternary, which is of technological interest as a possible material for high-k gate dielectric applications for Si microelectronics.[7,8] The substrates were introduced to the deposition chamber (base pressure lower than 7×10^{-4} Pa) through a load lock. They were then heated in vacuum to a deposition temperature of 400 °C, at which point O_2 flowed through the system to achieve a pressure of either 1.3 or 13.3 Pa. The substrate-target distance was set to ≈65 mm. Each film was deposited from a 2.54 cm, 99.99% pure ceramic target, with a raster of ±3° and a rotational speed of 60 °/s to ensure even target wear. The targets were well aged so that the deposition rate per laser pulse did not change significantly during the course of the deposition. Also, prior to deposition the laser entry window was cleaned with acetone and methanol to ensure that their energy losses during the growth were minimized. The beam energy was set to 300 mJ (which corresponds to a fluence of 15 J/cm^2), and the repetition rate was 20 Hz. The HfO_2, Al_2O_3, and Y_2O_3 targets were used for the 0°, 120°, and 240° substrate rotations, respectively. Each calibration film was grown using 10 000 laser pulses. After deposition, the samples were cooled to room temperature in vacuum.

In order to determine the thickness, we employed spectroscopic reflectometry. The spectroscopic reflectometer, de-

Downloaded 28 May 2008 to 129.6.180.72. Redistribution subject to AIP license or copyright; see http://rsi.aip.org/rsi/copyright.jsp

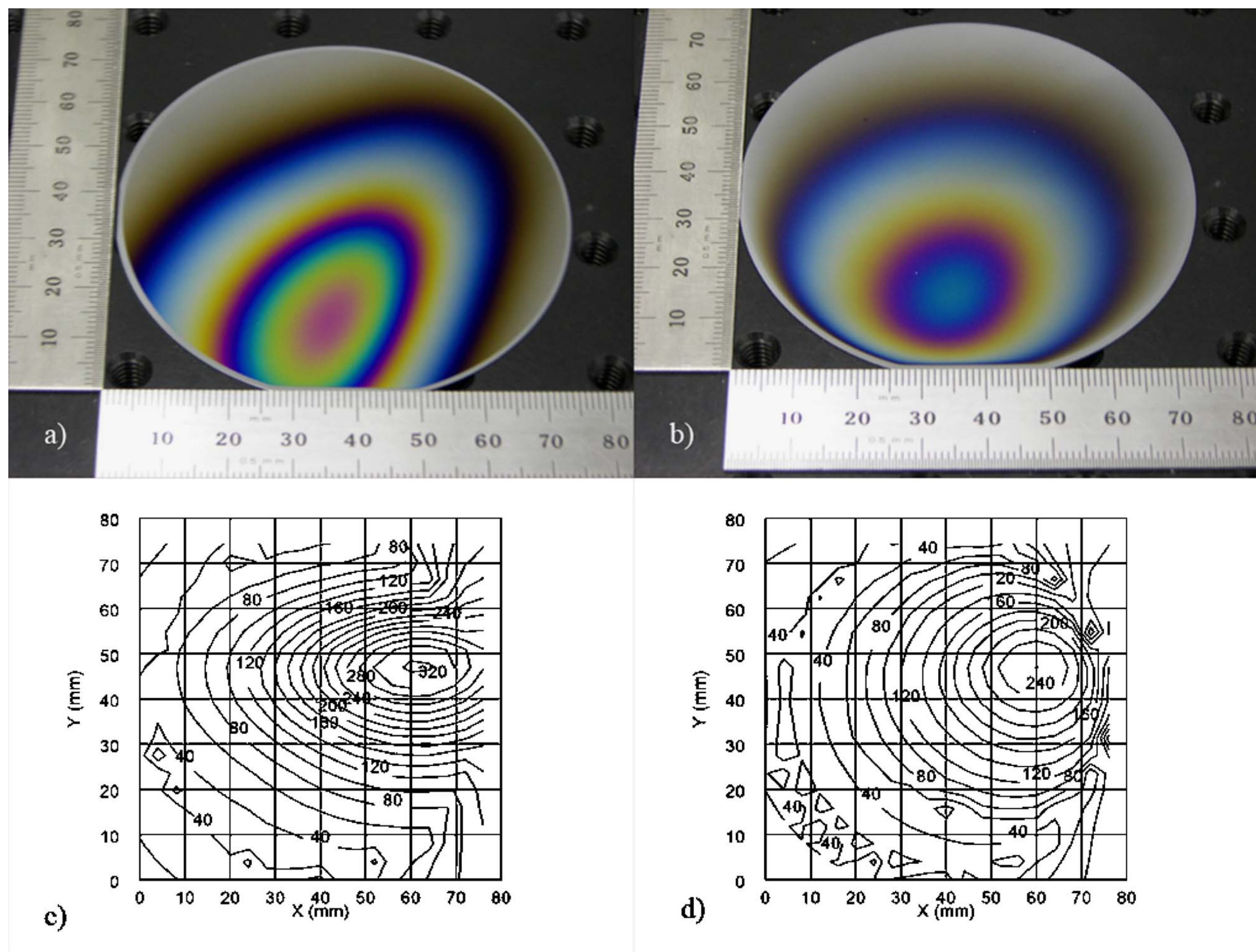

FIG. 2. (Color online) Single component calibration film of Y_2O_3 grown at (a) 1.3 Pa, (b) 13.3 Pa, and thickness contour plots rotated 120° for (c) 1.3 Pa and (d) 13.3 Pa.

scribed in detail elsewhere,[9] consists of a bifurcated fiber optic probe which both illuminates the film substrate and collects the reflected light, with 0.2 mm spatial resolution. The light source and spectrometer had a useful wavelength range of 400–950 nm. A bare silicon wafer is used as a reference to remove source and spectrometer response functions. Computer controlled *X-Y* stages were used to map the reflectivity of the film/substrate in a radial fashion (radius and angle) with roughly a 1 mm grid, resulting in over 4000 spectra for a 76.2 mm wafer. The resulting individual reflection spectra were fitted to a thin film interference model[10] using a nonlinear least squares algorithm.[11] Tabulated values[12] for the bulk indices of refraction (n and k) were used to fit the spectra. The resulting thickness map, for each target and pressure, is then fitted using our model [Eqs. (1)–(4)], allowing T_0, m, and n to vary. The center coordinates of the distribution, x_0 and y_0, were also allowed to vary. Since the data are obtained radially, it was straightforward to limit the model fit to the center of the substrate, thus avoiding edge effects.

After the films were fitted, we used the film growth rate data and thickness distribution to predict the composition and thickness of ternary libraries grown at 1.3 and 13.3 Pa. In order to determine composition, we employ mapping electron-probe microanalysis equipped with a wavelength-dispersive spectrometer (WDS). Samples are cut in half to fit into a WDS sample holder. Measurements were performed at 2 mm intervals. Compositions were calculated by comparison of x-ray fluorescence peak areas of samples with reference materials. Since WDS is sensitive to cation concentration, we focused on designing films that had an even flux of cations (Al, Hf, Y) at the (x_0, y_0) of each target in order to ensure maximal compositional coverage.

RESULTS

Figure 2 is a series of typical calibration Y_2O_3 films grown at 1.3 and 13.3 Pa oxygen pressure. Figures 2(a) and 2(b) are photographs of the actual films grown at 1.3 and 13.3 Pa, and Figs. 2(c) and 2(d) are thickness contour plots of Y_2O_3 obtained by reflectometry for each pressure. The contour plots are rotated 180° to make them easier to fit and compare on an *X-Y* grid. It is apparent from the shape of the deposited film that for the low-pressure case, $n > m$, and is similar to the shape of the laser spot, while for the case of the 13.3 Pa film, more scattering has occurred and n and m are closer to being equal, yielding a more symmetric deposition pattern.

The values of T_0, x_0, y_0, m, and n for each pressure and target material are presented in Table I. Movement of the

Downloaded 28 May 2008 to 129.6.180.72. Redistribution subject to AIP license or copyright; see http://rsi.aip.org/rsi/copyright.jsp

TABLE I. Thickness distribution data from calibration films. X coordinate and Y coordinate are measured relative to the ruler positions observed in Fig. 1.

Sample No.	Target material	Pressure (Pa)	Thickness at center T_0 (nm)	X coordinate at center x_0 (mm)	Y coordinate at center y_0 (mm)	Cosine distribution in x direction m	Cosine distribution in y direction n
1	HfO_2	1.3	256	64.0	39.6	7.75	29.0
2	HfO_2	13.3	190	61.0	38.8	9.0	18.4
3	Al_2O_3	1.3	258	57.0	49.0	5.7	11.6
4	Al_2O_3	13.3	184	52.8	46.3	7.6	9.65
5	Y_2O_3	1.3	327	62	45.4	6.5	18.1
6	Y_2O_3	13.3	250	59.0	45.0	8.0	12.5

center coordinates from target to target may be due to asymmetry of the system relative to the rotation axis (which is down the center of the wafer) and to a differences in the height of each target. Variation from center point to center point for a constant target may be attributable to a slight variation in wafer position due to the presence of slack between the wafer carrier and the wafer. We have estimated this rotational variation to be ±4.5°, although care is exercised during wafer loading to orient the wafer consistently within the wafer carrier.

It is also apparent from these data that the values of n are significantly lower for the case of 13.3 Pa. This is due to increased scattering of the plume due to an increased pressure of background gas. Values of m at high pressures are attributable to gas scattering, while the lower pressure values are a result of the rectangular beam shape. The 13.3 Pa values are consistent with literature values.[6] Finally, it is important to note that the thickness distribution is tighter (i.e., has a smaller angular range and higher values of n and m) for heavier species. The HfO_2 is affected least by background gases.

From these data, we were able to design combinatorial films and predict the thickness and compositional coverage for both 1.3 and 13.3 Pa combinatorial films. We designed combinatorial libraries so that they would have an even flux of cations at T_0 This involved a conversion of the thickness at $(x_0, y_0)_i$ to a molar fraction for each target, i, and equilibrating all of the targets to have a constant cation flux at that point. We also designed the experiment so that the thickest sublayer deposition was approximately 0.4 nm, to ensure complete mixing of the layers during film deposition. To convert from thickness to the number of moles of cation/laser pulse (MC), we employed the simple equation,

$$\mathrm{MC} = \frac{a_0}{N}\frac{\rho}{\mathrm{MW}}\mathrm{mol}_{\mathrm{cat}}, \tag{5}$$

where N is the number of laser pulses used in the calibration experiment, MW is the molecular weight of the target molecule, (ρ is the density of the species, and $\mathrm{mol}_{\mathrm{cat}}$ is the number of cation moles in the target compound. Table II is a list of experimental conditions for library growth that was determined using Eq. (5) in order to ensure even cation flux for each target in the library. The sublayer thickness of each pass is also calculated. The number of iterations pulse batch sets in the deposition was designed so that the thinnest part of the ternary would be ≈100 nm (at the Al_2O_3 site), since this is a thickness that is easy to fit by spectroscopic reflectometry.

Based on the data of Table I and the experimental design described in Table II, we were able to predict the thickness distribution in the film and the compositional coverage of the library. The thickness map was predicted in two ways. First, an addition of each individual calibration film thickness distribution for a composite map was carried out. The addition calibration film distribution has several advantages and one primary disadvantage. The advantages to summing raw distribution data is that asymmetry in the plume picture (i.e., when n is not symmetric around (x_0, y_0) because of gas flow effects around the wafer edge) is taken into account. However, any errors in fitting of the cosine power distribution

TABLE II. Deposition parameters for growth of $AlHfYO_x$ libraries at 1.3 and 13.3 Pa.

Pressure (Pa)	Iterations	Target material	Substrate position	Laser pulses in sublayer	Sublayer thickness (nm)
1.3	441	HfO_2	0	15	0.38
		Al_2O_3	120	9	0.23
		Y_2O_3	240	12	0.4
13.3	423	HfO_2	0	21	0.4
		Al_2O_3	120	17	0.24
		Y_2O_3	240	13	0.41

Downloaded 28 May 2008 to 129.6.180.72. Redistribution subject to AIP license or copyright; see http://rsi.aip.org/rsi/copyright.jsp

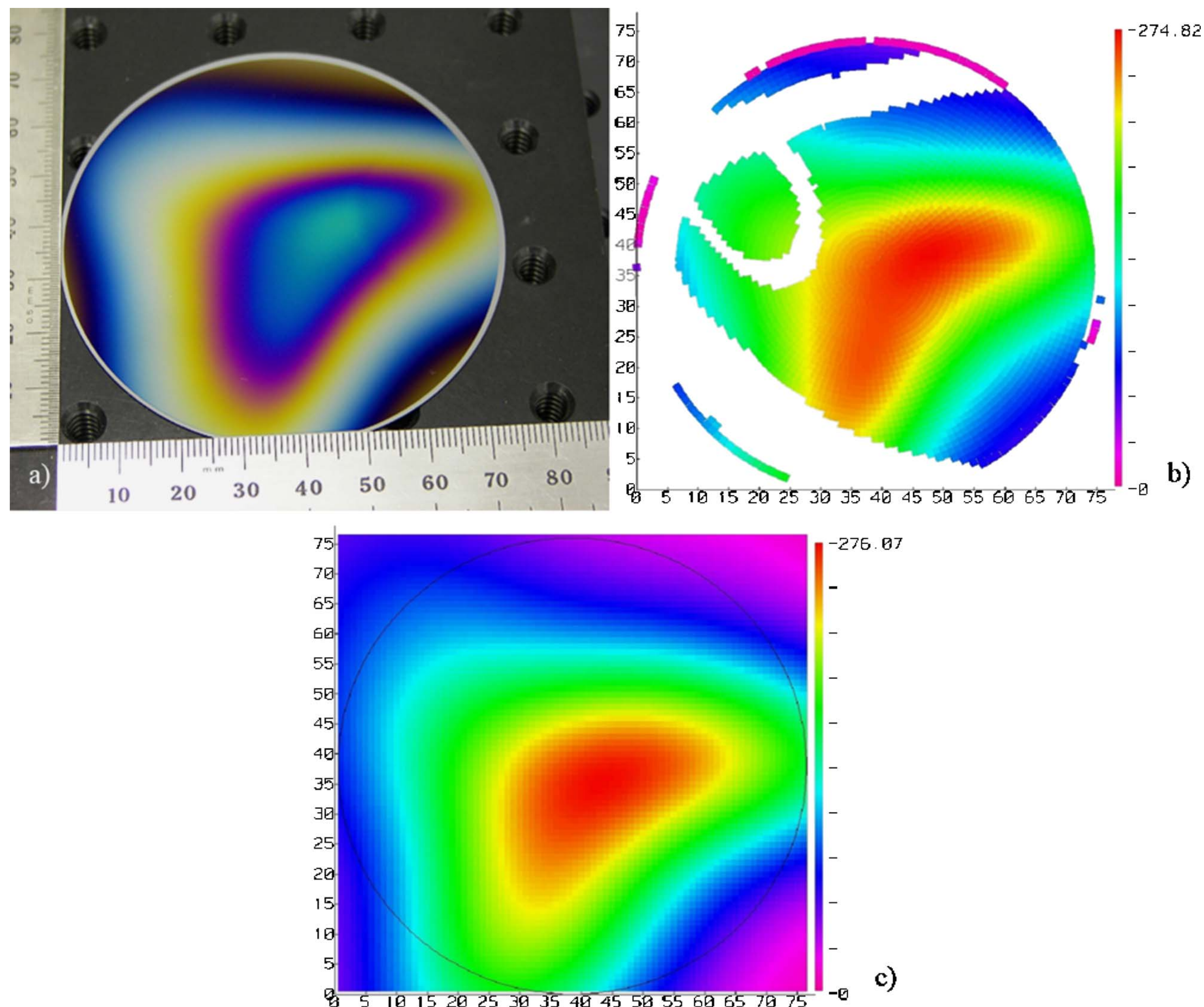

FIG. 3. (Color online) (a) Photograph of deposited 1.3 Pa library; (b) simulation of deposition pattern based on the sum of individual calibration spectra; (c) predicted bimodal cosine distribution pattern. The white areas in (b) correspond to missing information.

will not be taken into account. The primary disadvantage of using this method is that there is a potential loss of composition information if there are any errors in the original fitting of reflection data. Figure 3(a) is a demonstration of a predicted thickness map for the 1.3 Pa library film using the addition method. Places where information is lost are indicated in white. Second, Fig. 3(b) is a demonstration of the predicted thickness map using the cosine power fit with the appropriate values of m and n for each constituent target. The primary advantage of this fitting method is the translation of discrete data points with possible errors at specific points into a smooth analytical function. Nevertheless, the simplicity of the model does not take into account the gas flow and wafer edge effects and is mostly useful for predicting thickness and composition from each target toward the center of the wafer where the surface is planar and so has no gas flow effects which might affect plume shape. In addition, the use of an analytic function is desirable for designing experiments for optimizing uniformity or coverage, in which different geometrical parameters can be manipulated systematically.

Figures 4(a) and 4(b) compare the actual and simulated thickness distributions for the 13.3 Pa library sample. It should be noted that for both high- and low-pressure libraries, the shape of the thickness map closely resembles the thickness fringes coming from the deposited film. This implies that the predictive ability of the bimodal cosine power fit is a useful tool for predicting thickness distribution throughout the film. These predictions assume that there is no significant volume change as a function of composition. Of course, if there was a significant volume change (i.e., a new phase forms), it might lead to a change in refractive index, causing a discontinuity in the thickness fringes. A match of point-by-point x-ray data could be correlated to a refractive index change. In addition, the oxygen stoichiometry should be measured through another technique such as mapping x-ray photoelectron spectroscopy (XPS) to determine changes in oxygen coordination as the ratio of cations with different valences changes.

The ability to predict compositional coverage is very important for our simulations and design of experiment. Figure 5 shows, in a standard ternary compositional diagram representation, the simulated compositional coverage of the ter-

Downloaded 28 May 2008 to 129.6.180.72. Redistribution subject to AIP license or copyright; see http://rsi.aip.org/rsi/copyright.jsp

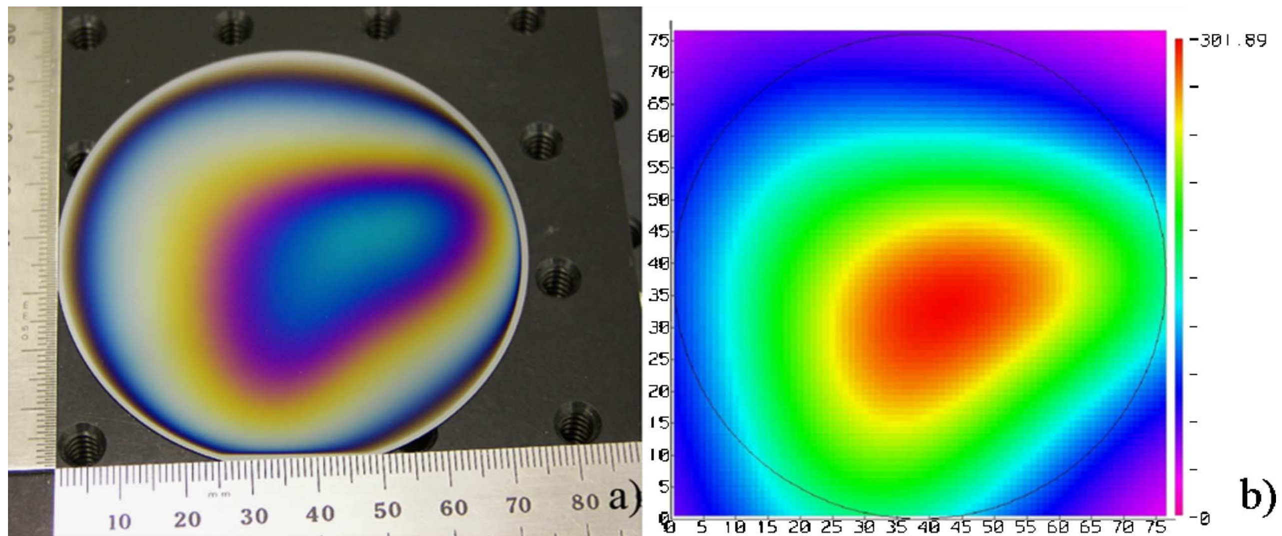

FIG. 4. (Color online) (a) Photograph and (b) predicted thickness map for library grown under 13.3 Pa conditions.

nary system as a function of pressure, compared to the compositional coverage from the WDS measurements. Each dot in the figure represents a predicted composition on the wafer for the simulations and an actual measurement from the WDS mapping. In these data, we can see several interesting phenomena. First, both the predicted and measured cation coverages show that the 13.3 Pa library has slightly more compositional coverage than the 1.3 Pa library. This is due to the increased symmetry of each single component plume. Secondly, we demonstrate that the predicted compositional coverage is quite accurate. Qualitatively, one can see that the WDS data have compositional coverage similar to the simulation.

In order to quantify this similarity, we calculated the linear correlation coefficient r^2, which relates the experimental data to the simulated data. The composition is calculated using the determined bimodal cosine distribution at each (X,Y) point of the WDS spatial map. The linear correlation coefficient is then calculated by assuming that the experimental data are a linear function of the simulation and vice versa. The product of the two slopes obtained is r^2. An r^2 value of 1 would be a perfect correlation. Since the calibration and WDS measurements are done with different instruments, there is a correction for rotational and translational alignments. The calculation is also limited to the central portion of the film (13–63 mm in both X and Y) where there are minimal edge effects due to gas flow. The value of r^2 for our WDS data and the simulation, after accounting for align-

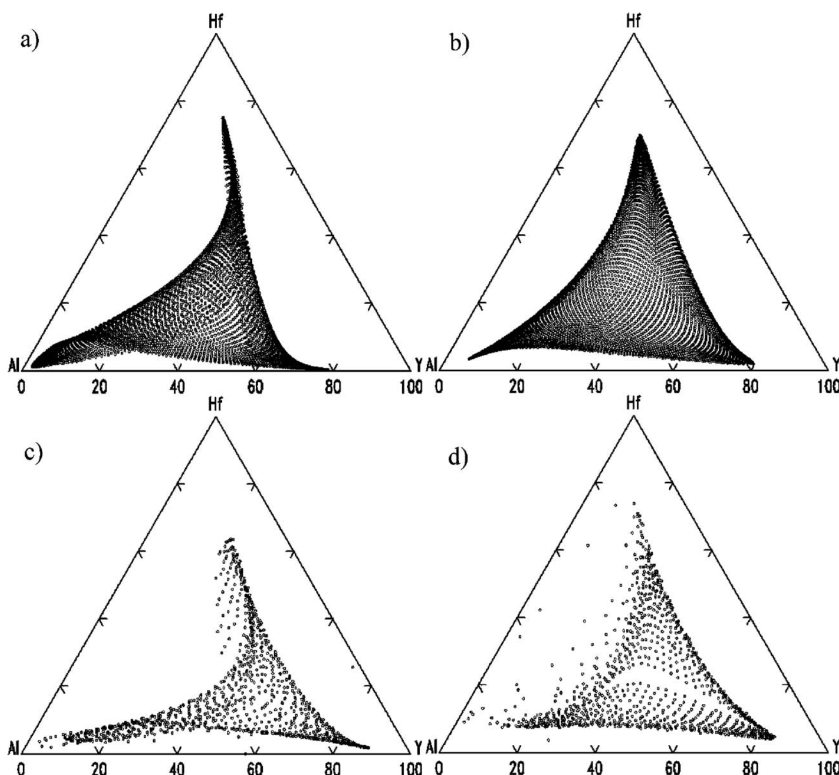

FIG. 5. Cation compositional coverage prediction based on the cosine model for (a) 1.3 Pa and (b) 13.3 Pa as well as the actual cation compositional coverage plotted on a ternary composition triangle for (c) 1.3 Pa and (d) 13.3 Pa. It is observed that the 13.3 Pa has a slightly larger cation concentration based on the increased plume symmetry. It can also be observed that the contours of the compositional measurement correlate well with the simulations. Finally, missing data in the experimental plot are due to wafer cleaving for WDS measurements.

Downloaded 28 May 2008 to 129.6.180.72. Redistribution subject to AIP license or copyright; see http://rsi.aip.org/rsi/copyright.jsp

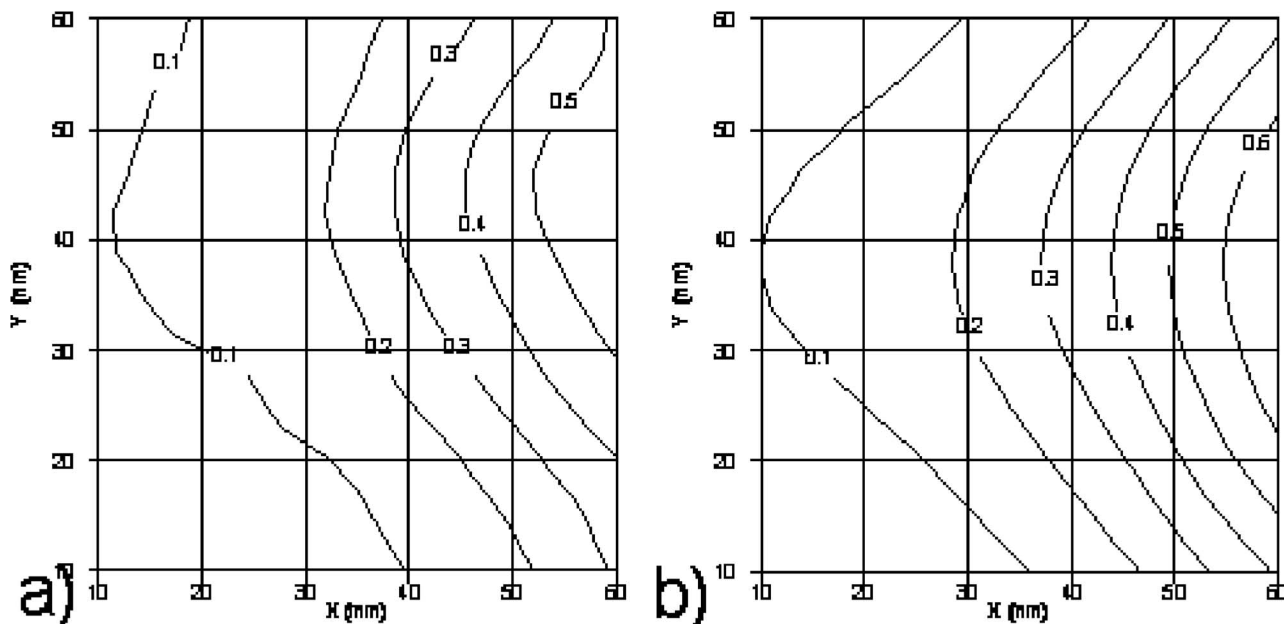

FIG. 6. Comparison of Hf mole fraction for the film deposited at 13.3 Pa O_2 as (a) determined by WDS measurements and (b) as simulated by the bimodal cosine distribution.

ment, is 0.98 for both the 1.3 and 13.3 Pa libraries, demonstrating an excellent correlation of the data and simulation in the center of the library film.

In addition, we sought to quantify the point-by-point comparison between predicted composition and measured composition. In Fig. 6, we demonstrate this comparison with side by side predicted and experimental mole fraction contour plots for Hf. There is a good agreement between the WDS composition measurements and the bimodal cosine simulations. The main differences between the two contour maps can be attributed to random (noise) and systematic (calibration) errors. The WDS determinations have random variations creating the noise in the contours. The thickness calibration relies on published values of the index of refraction and the density of bulk materials. There is certainly a variation from these numbers in the PLD deposited calibration films. In this work it results in a systematically high mole fraction prediction for the Hf and Al mole fractions and a lower prediction for the Y mole fraction as compared to the WDS measurements. In addition there is a slight rotation and translation of the coordinates of the WDS measurements from the thickness calibration coordinates. In spite of these limitations, the bimodal cosine simulations give a good first order indication of compositional coverage for the library films and aids in predicting changes in the coverage as deposition conditions are varied. One method to ensure greater accuracy of the thickness model is to perform spectroscopic ellipsometry on each calibration film to obtain a reliable index of refraction and absorption coefficient. We are currently incorporating that additional step into our experimental design.

The error associated with WDS measurements is higher than 1% per component. Since the measurement error is greater than the error associated with the correlation of our bimodal cosine distribution, we can conclude that this approximation is valid and useful for the estimation of thickness distribution and compositional coverage.

DISCUSSION

We have demonstrated that using a simple bimodal cosine power distribution function for the PLD deposition rate from three targets, we can predict the composition and thickness of ternary library films within WDS measurement accuracy. Thus, we can predict film composition and thickness with a high degree of confidence. This makes our model useful for routine library design, and costly experimental verification may be avoided for many applications.

[1] J. J. Hanak, J. Mater. Sci. **5**, 964 (1970).
[2] X. D. Xiang *et al.*, Science **268**, 1738 (1995).
[3] H. Koinuma and I. Takeuchi, Nat. Mater. **3**, 429 (2004).
[4] T. Fukumura *et al.*, Appl. Phys. Lett. **77**, 3426 (2000).
[5] H. M. Christen, S. D. Silliman, and K. S. Harshavardhan, Rev. Sci. Instrum. **72**, 2673 (2001).
[6] K. L. Saenger, in *Pulsed Laser Deposition of Thin Films*, edited by D. B. Chrisey and G. K. Hubler (Wiley, New York, 1994), Chap. 7, p. 199.
[7] G. D. Wilk, R. M. Wallace, and J. M. Anthony, J. Appl. Phys. **89**, 5243 (2001).
[8] K. Hasegawa, P. Ahmet, N. Okazaki, T. Hasegawa, K. Fujimoto, M. Watanabe, T. Chikyow, and H. Koinuma, Appl. Surf. Sci. **223**, 229 (2004).
[9] P. K. Schenck, D. L. Kaiser, and A. V. Davydov, Appl. Surf. Sci. **223**, 200 (2004).
[10] O. S. Heavens, *Optical Properties of Thin Solid Films*, 2nd ed. (Dover, New York, 1991).
[11] W. E. Wentworth, J. Chem. Educ. **42**, 162 (1965).
[12] E. D. Palik, *Handbook of Optical Constants of Solids II*, 3rd ed. (Academic, Boston, 1991).

Downloaded 28 May 2008 to 129.6.180.72. Redistribution subject to AIP license or copyright; see http://rsi.aip.org/rsi/copyright.jsp